24th COBEM - 2017

24th ABCM International Congress of Mechanical Engineering
December 3-8, 2017, Curitiba, PR, Brazil

COBEM-2017-2623
VISUAL SERVOING STABILIZATION OF A BALL AND PLATE MECHANISM BY USING AN ENHANCED DISTURBANCE REJECTION CONTROL METHOD

Alessandro Rosa Lopes Zachi
Sérgio Ramos Duarte Riveros
Pedro Paulo Pinheiro Lima
Centro Federal de Eduacação Tecnológica Celso Suckow da Fonseca - CEFET/RJ.
Electrical Engineering Program - Avenida Maracanã 229, Maracanã. CEP 20.271-110 - Rio de Janeiro, Brazil.
alessandro.zachi@cefet-rj.br, sergio.duarte@condornaoletal.com.br, pppl@yahoo.com.br

Josiel Alves Gouvêa
Centro Federal de Eduacação Tecnológica Celso Suckow da Fonseca - CEFET/RJ.
Research Nucleus on Mechatronics - Estr. de Adrianópolis 1317, Santa Rita, Nova Iguaçu. CEP 26.041-271 - Rio de Janeiro, Brazil.
josiel.gouvea@cefet-rj.br

Antonio Candea Leite
Pontifice Catholic University of Rio de Janeiro - PUC-Rio.
Department of Electrical Engineering (DEE) - Rua Marquês de São Vicente 225, Gávea. CEP 22.451-900 - Rio de Janeiro, RJ - Brazil.
antonio@ele.puc-rio.br

Abstract. *This work describes a controller synthesis for the stabilization of a ball and plate system by using visual servoing technique. The mechanism is composed by a free rolling ball that moves on a flat plate fixed in its center. The plate tilting angles are driven by two direct-current (dc) motors physically attached to the X and Y axis of the plate. For the measurement of the controlled variable, i. e., the ball cartesian position, a stationary CCD camera is used. The proposed solution for the visual servoing controller is based on the formalism of the Active Disturbance Rejection Control (ADRC) aiming to account for the parametric uncertainties of the system camera-mechanism-motors. Simulation results are presented to illustrate the behavior of the closed-loop system.*

Keywords: *Ball and Plate mechanism, visual servoing, ADRC, uncertain parameters.*

1. INTRODUCTION

The ball and plate balacing system presents a challenging control design problem due to the inherent complexity in its dynamical equations. The study of such system in academia has been an object of constant interest in recent years since its solutions can be used in many applications today. Some examples are: mechanism for flight simulation (Mauro *et al.*, 2016), Stewart platform (Kumar *et al.*, 2017), solar tracker (Wu *et al.*, 2016) and pick-and-place applications (Liao *et al.*, 2013). As can be verified from reports in the literature (Galvan-Colmenares *et al.*, 2014) a large number of control proposals have been previously implemented on real ball and plate systems. For example, reports on the utilization of Sliding-Mode Control in (Park and Lee, 2003), Active-Disturbance Rejection Controller (ADRC) in (Rubio *et al.*, 2014), fuzzy logic in (Liu and Yu, 2012) and Linear Quadratic Regulator (LQR) control algorithm in(Cheng and Tsai, 2016). As can be noticed in the cited works and from the references therein, the compensation for uncertainties of model parameters have been of concern since the early developments, in an attempt to circumvent the performance degradation particularly regarding the mechanism's and camera calibration parameters.

2. PROBLEM STATEMENT

In this work, a stabilization control solution for the ball and plate mechanism is developed. The control aim is keep the ball stabilized in a desired (fixed) position on the plate by actuating on the voltages of two armature-controlled DC motors which are responsible for tilting the angles $\alpha \in \mathbb{R}$ and $\beta \in \mathbb{R}$, as depicted on Fig. 2. To measure the cartesian position of the ball on the plate, a fixed CCD camera is used. In order to incorporate the dynamics of the motors as well as

the camera projection model into the overall equations of motion of the mechanism, additional time differentiation steps are made on the original dynamics traditionally considered in the literature. This way, the control variables, i.e., the input voltages for the motors become explicit related to the controlled variables $[x_c, y_c]^T \in \mathbb{R}^2$ which defines the ball cartesian position in image coordinates. Although the knowledgement of such dynamical relantionships is desired for the controller design, the system complexity increases and additional parametric uncertainties arise in the resulting model.

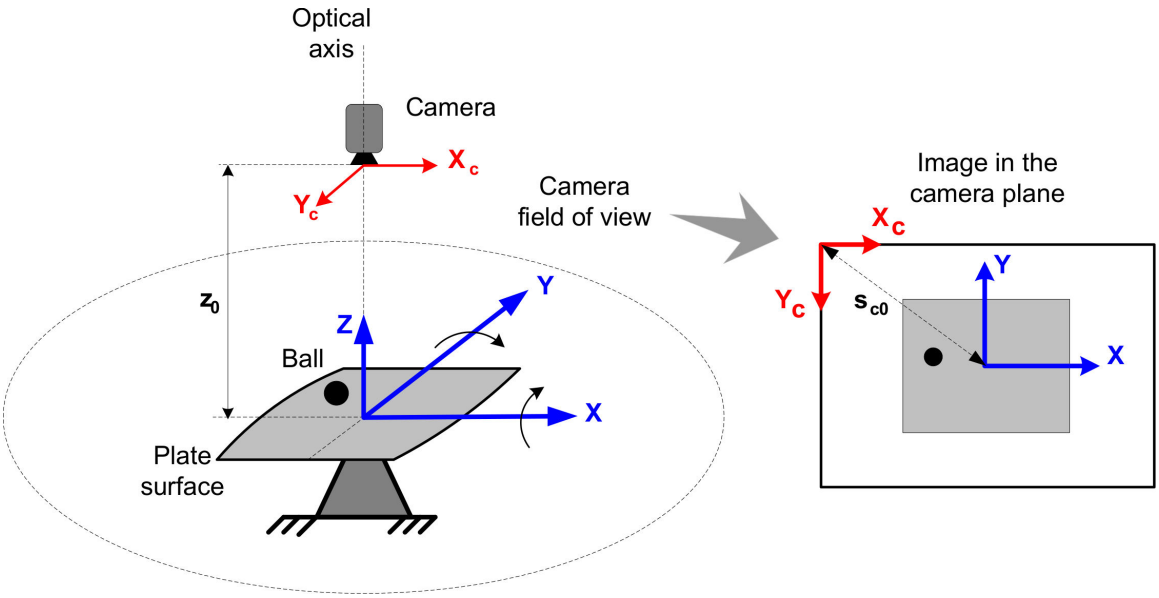

Figure 1: Illustrative Diagram of the Visual Serving Ball and Plate system.

3. METHODOLOGY

To solve the problem of controlling the mechanism, in the presence of parametric uncertainties of the dynamical model, we developed a modified version of the Active Disturbance Rejection Method (ADRC) (Han, 1998; Gao *et al.*, 2001; Han, 2009). It consists basically of an extended observer that estimates the system states and non-measurable signals that act together with a state feedback control law. In the present proposed method we perform slight modifications both on the input/output dynamics of the plant and on the observer equations that brings some mathematics advantages that will be useful in the design of the closed-loop controller. Theoretical contributions of the proposed control strategy that we may cite are: (i) the exact knowledgement of system parameters, i. e., camera intrinsic parameters and motor's electromechanical constants are not required; (ii) the control synthesis is simplified due to the use of a reduced set of design constants; (iii) complexity is reduced due to the use of linear structures both on the observer and on the control law design.

4. SYSTEM MODEL

In this section, the Ball and Plate dynamical equations are obtained by using the Langrangian Formalism as in (Fan *et al.*, 2004; Lee *et al.*, 2008; Yuan and Zhang, 2010):

$$\frac{d}{dt}\frac{\partial T}{\partial \dot{q}_i} - \frac{\partial T}{\partial q_i} + \frac{\partial V}{\partial q_i} = Q_i \,, \tag{1}$$

in which $q_i \in \mathbb{R}$ stands for i-th direction coordinate, $T \in \mathbb{R}$ is kinetic energy of the system, $V \in \mathbb{R}$ is potential energy of system and $Q \in \mathbb{R}$ is composite force. Since both the ball displacement and the plate orientation are bi-dimensional, the overall mechanism has four degrees of freedom. In the following model development, we define the generalized coordinates of the overall system as $[x, y]^T$ (the ball cartesian position) and α, β (the plate tilting angles). We also consider that the origin of the ball coordinated axis is fixed in the center of the plate as depicted in Fig. 2. Regarding at model simplification, the following assumptions are assumed:

(H1) The ball does not loose contact with the plate during motion;

(H2) The ball motion is such that no slipping occurs;

(H3) The ball is a homogeneous rigid body with a symmetric geometry.

After applying the Lagrangian formulas, as was done in (Yuan and Zhang, 2010), the equations of motion result in:

$$\begin{aligned}\left(m+\frac{I_b}{m}\right)\ddot{x}-m(x\dot{\alpha}^2+y\dot{\alpha}\dot{\beta})+mg\ sin(\alpha)\ &=\ 0\,,\\ \left(m+\frac{I_b}{m}\right)\ddot{y}-m(y\dot{\beta}^2+x\dot{\alpha}\dot{\beta})+mg\ sin(\beta)\ &=\ 0,\end{aligned} \tag{2}$$

in which $x(t), y(t) \in \mathbb{R}$ are the ball displacements $[meter]$ over the plate surface in X and Y directions, respectively; $\alpha(t)\,, \beta(t) \in \mathbb{R}$ are the plate tilt angles $[rad]$ around the Y and X axis, respectively; m is the ball mass $[Kg]$; I_b is the ball inertia $[Kg.m^2]$ and g is the gravity acceleration constant $[m/s^2]$. Since the approximate value for the ball's moment of inertia is given by $I_b = 2mr_b^2/5$, the expressions in Eq. (3) can be simplified to

$$\frac{5}{7}\ddot{x}-(x\dot{\alpha}^2+y\dot{\alpha}\dot{\beta})+g\ sin(\alpha)\ =\ 0\,,\qquad \frac{5}{7}\ddot{y}-(y\dot{\beta}^2+x\dot{\alpha}\dot{\beta})+g\ sin(\beta)\ =\ 0\,. \tag{3}$$

Since a CCD camera is used to measure the ball position, its projection model need to be included in the above system equation. In this work, we consider that the camera is mounted in a fixed depth position z_0 along the plate's Z axis. We also assume that the camera's optical axis is parallel to the plate's Z axis and the z_0 value is sufficient to focuses the plane's center and its borders. Such configuration can be observed in Fig. 2. Thus, if we denote the ball image coordinates as x_c, y_c [pixels], then by adopting perspective projection model (Haralick and Shapiro, 1993) the relationship between cartesian coordinates [meters] and image coordinates [pixels] can be given by:

$$x_c=\left(\frac{\lambda f}{z_0}\right)x+x_{c0}\,,\qquad y_c=-\left(\frac{\lambda f}{z_0}\right)y+y_{c0}\,, \tag{4}$$

in which $f \in \mathbb{R}$ is the value of the camera focal length $[meter]$ and $\lambda \in \mathbb{R}$ is the meter-to-pixel transformation factor. The constants $x_{c0}, y_{c0} \in \mathbb{R}$ are used in Eq. (4) to account for the translational displacement between the cartesian coordinate system and the camera coordinate system. Observing that $\lambda f/z_0$ is constant, the incorporation of Eq. (4) in the model of Eq. (3) results in

$$\begin{aligned}&\ddot{x}_c-K_1[(x_c-x_{c0})\dot{\alpha}^2+(y_c-y_{c0})\dot{\alpha}\dot{\beta}]+K_2 sin(\alpha)\ =\ 0\,,\\ &\ddot{y}_c-K_1[(y_c-y_{c0})\dot{\beta}^2+(x_c-x_{c0})\dot{\alpha}\dot{\beta}]-K_2 sin(\beta)\ =\ 0\,,\\ &K_1=\frac{7}{5}\,,\qquad K_2=\left[\frac{7g\lambda f}{5z_0}\right]\,,\end{aligned} \tag{5}$$

which consists on the plant dynamics described in terms of image coordinates. As can be noticed, the control variables, namely, the input voltages for the tilting motors, are not explicitly present in the expressions of Eq. (5). For this reason, the motors' equations of motion need to be introduced in the present system modeling. The DC motors considered in this paper are armature voltage driven. Their dynamics of motion can be found in many control textbooks (Dorf, 2008). In the following, we present the dynamics of motor α :

$$\frac{\alpha(s)}{V_\alpha(s)}=\frac{K_m}{s[(R_a+sL_a)(Js+B)+K_mK_b]}\ \approx\ \frac{K_m}{s[(R_a)(Js+B)+K_mK_b]}\,, \tag{6}$$

being K_m the motor torque constant $[N.m/A]$, K_b the back-emf constant $[V.s/rad]$; J_m the rotor inertia $[N.M.s^2/rad]$; B the rotor damping factor $[N.m/(rad/s)]$; R_a the armature resistance $[\Omega]$ and L_a the armature inductance $[H]$. In general, the armature inductance value L_a is three orders of magnitude smaller than the value of the armature resistance. In this case, the term $(R_a + sL_a)$ can be replaced by (R_a), without loss of generality and then, the motor dynamics reduces to the one on the right-hand side of Eq. (6). For motor β, the model is similar but with minor differences:

$$\frac{\beta(s)}{V_\beta(s)}=\frac{\bar{K}_m}{s[(\bar{R}_a)(\bar{J}s+\bar{B})+\bar{K}_m\bar{K}_b]}\,. \tag{7}$$

The models in Eqs. (6) and (7) can also be represented in time domain as:

$$\ddot{\alpha}=-\left(\frac{R_aB+K_mK_b}{JR_a}\right)\dot{\alpha}+\left(\frac{K_m}{JR_a}\right)V_\alpha\,,\qquad \ddot{\beta}=-\left(\frac{\bar{R}_a\bar{B}+\bar{K}_m\bar{K}_b}{\bar{J}\bar{R}_a}\right)\dot{\beta}+\left(\frac{\bar{K}_m}{\bar{J}\bar{R}_a}\right)V_\beta\,. \tag{8}$$

Thus, to take advantages of the formulation of Eq. (8), we need to linearize Eq. (5). For this purpose, we consider the occurrence of small tilting angles $\alpha = \pm 5^o = 0.087\ rad$ and $\beta = \pm 5^o = 0.087\ rad$, such that $sin(\alpha) = \alpha$, $sin(\beta) = \beta$.

Also, we assume sufficiently small tilting velocities $\alpha << 0$ and $\beta << 0$. From last hypothesis, the quadratic and crossed terms involving $\dot{\alpha}$ and $\dot{\beta}$ can be neglected, i.e., $\dot{\alpha}^2 \approx 0$, $\dot{\alpha}\dot{\beta} \approx 0$ and $\dot{\beta}^2 \approx 0$, and then Eq. (5) becomes:

$$\ddot{x}_c = -K_2\alpha\,, \qquad \ddot{y}_c = K_2\beta\,. \tag{9}$$

Then, by taking the second order time derivatives of the expressions in Eq. (9), based on Eq. (8), we finally achieve the dynamical model for the plant:

$$\begin{aligned} \dddot{x}_c &= \underbrace{K_2\left(\frac{R_aB + K_mK_b}{JR_a}\right)}_{\rho_1}\dot{\alpha} + \underbrace{\left(\frac{-K_2\,K_m}{JR_a}\right)}_{\sigma_1}V_\alpha \qquad \longrightarrow \qquad \dddot{x}_c = \rho_1\dot{\alpha} + \sigma_1 V_\alpha\,, \\ \dddot{y}_c &= \underbrace{K_2\left(\frac{\bar{R}_a\bar{B} + \bar{K}_m\bar{K}_b}{\bar{J}\bar{R}_a}\right)}_{\rho_2}\dot{\beta} + \underbrace{\left(\frac{K_2\,\bar{K}_m}{\bar{J}\bar{R}_a}\right)}_{\sigma_2}V_\beta \qquad \longrightarrow \qquad \dddot{y}_c = \rho_2\dot{\beta} + \sigma_2 V_\beta\,. \end{aligned} \tag{10}$$

5. CONTROL DESIGN VIA TRADITIONAL ADRC METHOD

In this section, the position control of the ball and plate system described by Eq. (10) is addressed. In this work, we adopt the *Active Disturbance Rejection Control* (ADRC) method (Han, 1998; Gao *et al.*, 2001; Han, 2009; Xue *et al.*, 2015; Xia *et al.*, 2016) to deal with model uncertanties. It is important to point out that such uncertainties may occur in the plant parameters in (10) in particular due to the lack of exact knowledgement of motor's constants and of camera intrinsic parameters therein.

For the sake of simplicity and also due to the similarity of the expressions in Eq.(10), the control design will be carried out only considering the state variable $x_c(t)$. Following the design procedures discussed in (Han, 1998; Gao *et al.*, 2001; Han, 2009), the $x_c(t)$ dynamics can be rewritten in the format:

$$\dddot{x}_c = h(t) + \sigma_1 V_\alpha\,, \qquad h(t) = \rho_1\dot{\alpha}\,. \tag{11}$$

In (Han, 1998; Gao *et al.*, 2001; Han, 2009), the function $h(t)$ is denoted by *generalized disturbance term* and represents a combination of the non measurable signals of the system. As part of the traditional formalism, the control law the control V_α is chosen as:

$$V_\alpha = \left(\frac{1}{\sigma_1}\right)\left[-\hat{h}(t) - d_3\dddot{\hat{x}}_c - d_2\ddot{\hat{x}}_c - d_1\dot{\hat{x}}_c - d_0\hat{x}_c + d_0\hat{x}_c^*\right], \tag{12}$$

in which $\hat{x}_c^* \in \mathbb{R}$ is the set-point coordinate in the image, $d_3,\ d_2,\ d_1,\ d_0\ \in \mathbb{R}$ are the coeficients of a monic and stable polinomial of order 4, and $\hat{\mathbf{Z}} = [\hat{h}(t);\ \dddot{\hat{x}}_c;\ \ddot{\hat{x}}_c;\ \dot{\hat{x}}_c;\ \hat{x}_c]^T$ represent the estimate of vector $\mathbf{Z} = [h(t);\ \dddot{x}_c;\ \ddot{x}_c;\ \dot{x}_c;\ x_c]^T$, generated by an *extended state observer* (ESO) of the form:

$$\begin{aligned} \dot{\hat{\mathbf{Z}}} &= \begin{bmatrix} 0 & 1 & 0 & 0 & 0 \\ 0 & 0 & 1 & 0 & 0 \\ 0 & 0 & 0 & 1 & 0 \\ 0 & 0 & 0 & 0 & 1 \\ 0 & 0 & 0 & 0 & 0 \end{bmatrix}\hat{\mathbf{Z}} - \begin{bmatrix} 0 \\ 0 \\ 0 \\ \sigma_1 \\ 0 \end{bmatrix}u + \underbrace{\begin{bmatrix} L_1 \\ L_2 \\ L_3 \\ L_4 \\ L_5 \end{bmatrix}}_{\mathbf{L}}e_y\,, \\ \hat{w} &= \begin{bmatrix} 1 & 0 & 0 & 0 & 0 \end{bmatrix}\hat{\mathbf{Z}}\,, \end{aligned} \tag{13}$$

In the observer plant of Eq. 13, $\mathbf{L} = [L_1; L_2; L_3; L_4; L_5]^T$ represents the vector of observer gains and $\hat{w} \in \mathbb{R}$ represents the observer output signal. The observer-based control scheme of ADRC method is illustrated in the diagram of Fig. 2

Remark 1 *As can be verified from the previous developments, the designs of the control law of Eq. (12) and of the ESO of Eq. (13) are dependent on the exact knowledgement of the control gain σ_1. Such design difficulty has been avoided in several ADRC schemes by assuming that σ_1 is completely or partially known a priori (Han, 1998; Gao* et al.*, 2001; Han, 2009; Madoński and Herman, 2011; Zhu* et al.*, 2014; Xue* et al.*, 2015; Xia* et al.*, 2016). Contrasting with the strategies proposed on the cited works, in the present paper we introduce a modified ADRC framework in order to deal with uncertainties within the parameter σ_1.*

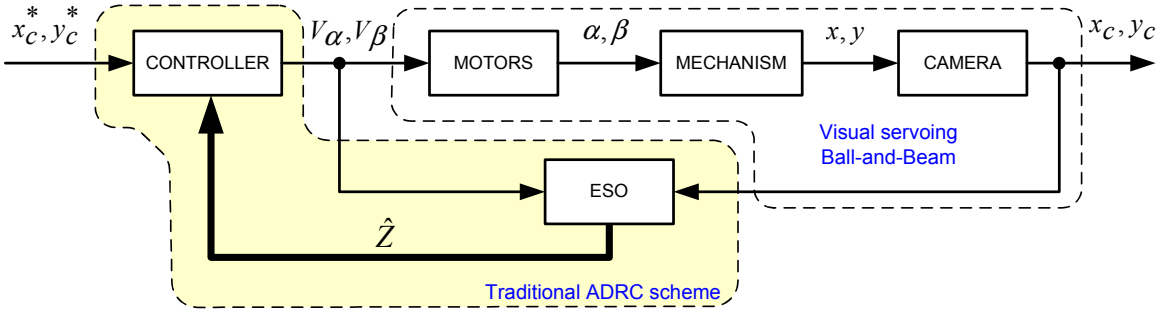

Figure 2: Illustrative Diagram of the traditional ADRC scheme.

6. CONTROL DESIGN USING AN ENHANCED ADRC METHOD

In order to deal with the parametric uncertainties that appear in the control gain σ_1 of Eq. (11), a modified version of the *Active Disturbance Rejection Control* approach will be introduced. The main idea of the proposal is to introduce a structural transformation in the input/output description of the original system, in order to obtain a new dynamical equation with a known control gain. Once it has been achieved, then the ADRC method will be applied to the transformed system without restrictions. The proposal to produce the cited transformation consists in the introduction of a constant gain K_s cascaded with the plant output and a forth order linear (stable) filter $Q_0(s)$ in parallel with the overall input/output model, as depicted in Fig. 3.

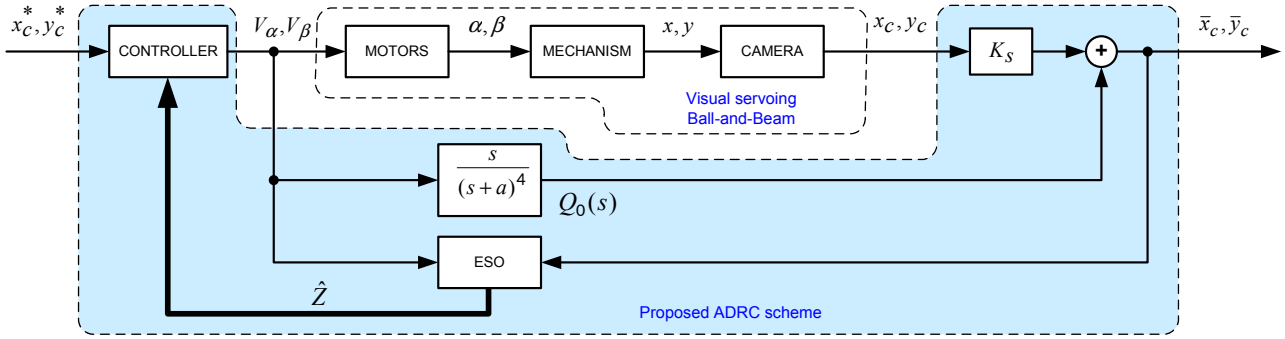

Figure 3: Illustrative Diagram of the Enhanced ADRC proposed in the present work.

As will be shown, the proposed scheme will perform slight modifications on the input/output plant description that will not affect the control objectives outlined for the original plant and, also, will bring out some useful mathematical properties for the control design.

6.1 Control law definition

In time domain, the output variable $\bar{x}_c$ of the transformed plant is defined by:

$$\begin{aligned} \bar{x}_c &= K_s\, x_c + V_{\alpha f}\,, \\ Q_0(s) \;:\; \dddot{V}_{\alpha f} &= -\gamma_3 \ddot{V}_{\alpha f} - \gamma_2 \dot{V}_{\alpha f} - \gamma_1 \dot{V}_{\alpha f} - \gamma_0 V_{\alpha f} + \dot{V}_\alpha\,, \end{aligned} \tag{14}$$

in which $\gamma_3,\ \gamma_2,\ \gamma_1,\ \gamma_0$ are coeficients of the polinomial $(s+a)^4$, and $V_{\alpha f} \in \mathbb{R}$ is the filtered version of the control signal V_α, generated in the output of the filter $Q_0(s)$ in Fig. 3.

By differentiating the signal $\bar{x}_c$ of Eq. (14) four times, the dynamics of the transformed system will be given by:

$$\ddddot{\bar{x}}_c = K_s\rho_1\dot{\alpha} + \underbrace{K_s\sigma_1 V_\alpha - \gamma_3 \dddot{V}_{\alpha f} - \gamma_2 \ddot{V}_{\alpha f} - \gamma_1 \dot{V}_{\alpha f} - \gamma_0 V_{\alpha f} + \dot{V}_\alpha}_{\zeta(t)}\,. \tag{15}$$

In the present work, the design constant K_s is defined as

$$K_s := k_0\; sign(\sigma_1)\,, \quad k_0 > 0 \in \mathbb{R}\,. \tag{16}$$

Based on Eq. (15) and Eq. (16), the frequency domain expression for $V_\alpha(s)$ is given by:

$$sV_\alpha(s) = -k_0|\sigma_1|V_\alpha(s) - \left[\frac{(\gamma_3 s^4 + \gamma_2 s^3 + \gamma_1 s + \gamma_0)s}{s^4 + \gamma_3 s^3 + \gamma_2 s^2 + \gamma_1 s + \gamma_0}\right] V_\alpha(s) + \zeta(s) \;=\; -(k_0|\sigma_1| + \gamma_3)\times$$
$$\times \underbrace{\left[\frac{s^4 + \left(\frac{k_0|\sigma_1|\gamma_3+\gamma_2}{k_0|\sigma_1|+\gamma_3}\right)s^3 + \left(\frac{k_0|\sigma_1|\gamma_2+\gamma_1}{k_0|\sigma_1|+\gamma_3}\right)s^2 + \left(\frac{k_0|\sigma_1|\gamma_1+\gamma_0}{k_0|\sigma_1|+\gamma_3}\right)s + \left(\frac{k_0|\sigma_1|\gamma_0}{k_0|\sigma_1|+\gamma_3}\right)}{s^4 + \gamma_3 s^3 + \gamma_2 s^2 + \gamma_1 s + \gamma_0}\right]}_{c_0} V_\alpha(s) + \zeta(s) \tag{17}$$

$$sV_\alpha(s) = -\underbrace{[(k_0|\sigma_1| + \gamma_3)c_0]}_{c_1} V_\alpha(s) + \zeta(s)\,, \tag{18}$$

in which $c_0 > 0 \in \mathbb{R}$ is dummy variable introduced only for analysis purpose. Thus, adopting a sufficiently large value for k_0 in Eq. (16), then the variable c_0 on the right-hand side of Eq. (17) will become sufficiently close to the unit value. Once we know that $k_0,\ \gamma_3,\ c_0$ are positive, we guarantee that constant c_1 in Eq. (18) will be positive which implies that $V_\alpha(t)$ will be bounded for every bounded $\zeta(t)$, i. e.,

$$V_\alpha(s) = \left(\frac{1}{s + c_1}\right) \zeta(s)\,. \tag{19}$$

Thus, based on Eq. (19), the Eq. (15) assumes a more simple format, namely:

$$\dddot{\bar{x}}_c = K_s\rho_1\dot{\alpha} + \underbrace{c_1 V_\alpha + \dot{V}_\alpha}_{\zeta(t)}\,. \tag{20}$$

Now, adopting the ADRC formalism to rewrite Eq. (20), we obtain:

$$\begin{cases} \dddot{\bar{x}}_c = \psi(t) + \dot{V}_\alpha\,, \\ \psi(t) = K_s\rho_1\dot{\alpha} + c_1 V_\alpha\,. \end{cases} \tag{21}$$

Under the new framework, the control law is defined by the signal $\dot{V}_\alpha$. Now, the ADRC method can be applied without restriction because the term $\dot{V}_\alpha$ has unitary control gain. Based on Eq. (12), the control law for the plant (21) can be chosen as

$$\dot{V}_\alpha = -\hat{\psi}(t) - d_3\dddot{\hat{\bar{x}}}_c - d_2\ddot{\hat{\bar{x}}}_c - d_1\dot{\hat{\bar{x}}}_c - d_0\hat{\bar{x}}_c + d_0\bar{x}_c^*\,, \tag{22}$$

being $\bar{x}_c^* = K_s x_c^*$ the modified set-point value and $\hat{\bar{\mathbf{Z}}} = [\dddot{\hat{\bar{x}}}_c,\ \ddot{\hat{\bar{x}}}_c,\ \dot{\hat{\bar{x}}}_c,\ \hat{\bar{x}}_c, \hat{\psi}(t)]^T$ the vector of estimated states whose dynamics are governed by the ESO:

$$\dot{\hat{\bar{\mathbf{Z}}}} = \underbrace{\begin{bmatrix} 0 & 1 & 0 & 0 & 0 \\ 0 & 0 & 1 & 0 & 0 \\ 0 & 0 & 0 & 1 & 0 \\ 0 & 0 & 0 & 0 & 1 \\ 0 & 0 & 0 & 0 & 0 \end{bmatrix}}_{\mathbf{A}} \hat{\bar{\mathbf{Z}}} + \underbrace{\begin{bmatrix} 0 \\ 0 \\ 0 \\ 1 \\ 0 \end{bmatrix}}_{\mathbf{B}} \dot{V}_\alpha + \underbrace{\begin{bmatrix} L_1 \\ L_2 \\ L_3 \\ L_4 \\ L_5 \end{bmatrix}}_{\mathbf{L}} e_{\bar{w}}\,,$$
$$\hat{\bar{w}} = \underbrace{\begin{bmatrix} 1 & 0 & 0 & 0 & 0 \end{bmatrix}}_{\mathbf{C}} \hat{\bar{\mathbf{Z}}}\,, \tag{23}$$
$$e_{\bar{w}} = \bar{w} - \hat{\bar{w}}\,.$$

Defining

$$\bar{\mathbf{e}}_x := \bar{\mathbf{Z}} - \hat{\bar{\mathbf{Z}}}\,, \tag{24}$$

and supposing that $\psi(t)$ is differentiable, the observer error dynamics will be given by:

$$\dot{\bar{e}}_x = \underbrace{\begin{bmatrix} -L_1 & 1 & 0 & 0 & 0 \\ -L_2 & 0 & 1 & 0 & 0 \\ -L_3 & 0 & 0 & 1 & 0 \\ -L_4 & 0 & 0 & 0 & 1 \\ -L_5 & 0 & 0 & 0 & 0 \end{bmatrix}}_{(\mathbf{A}-\mathbf{LC})} \bar{\mathbf{e}}_x + \underbrace{\begin{bmatrix} 0 \\ 0 \\ 0 \\ 0 \\ 1 \end{bmatrix}}_{\Lambda} \dot{\psi}(t)\,,$$
$$\bar{e}_w = \begin{bmatrix} 1 & 0 & 0 & 0 & 0 \end{bmatrix} \bar{\mathbf{e}}_x\,. \tag{25}$$

6.2 Observer convergence

In order to study the influence of the generalized disturbance $\psi(t)$ in the convergence of the observer estimates $\hat{\bar{\mathbf{Z}}}$ in Eq. (23), let us analyse the input/output relationships of Eq. (25) regarding $\dot{\psi}(t)$ as an input in standard form and the state variables $\hat{Z}_1, \hat{Z}_2, \hat{Z}_3, \hat{Z}_4, \hat{Z}_5$, one at a time, as the system output, i.e.,

$$\begin{aligned} &\frac{\bar{E}_{xi}(s)}{s\Psi(s)} = \mathbf{C}_i[sI - (\mathbf{A} - \mathbf{LC})]^{-1}\mathbf{\Lambda}\,, \quad s\Psi(s) = \mathcal{L}\left\{\dot{\psi}(t)\right\}\,, \quad \bar{E}_{xi}(s) = \mathcal{L}\left\{\bar{e}_{xi}(t)\right\} \\ &\bar{e}_{xi} = \mathbf{C_i}\bar{\mathbf{e}}_{\mathbf{x}}\,, \quad (i = 1, \cdots, 4)\,. \end{aligned} \tag{26}$$

In Eq. (26), $\mathbf{C_i}$ accounts for the choice of the error variable, for instance, for $\bar{e}_{x1}$ one may assign $\mathbf{C}_i = \mathbf{C}_1 = [1\,0\,0\,0\,0]$, for $\bar{e}_{x2}$ one may assign $\mathbf{C}_i = \mathbf{C}_2 = [0\,1\,0\,0\,0]$ and so on. Then, by using Eq. (26), we obtain the following relationships:

$$\begin{aligned} &\frac{\bar{E}_{x1}(s)}{s\Psi(s)} = \frac{1}{s^5 + L_1s^4 + L_2s^3 + L_3s^2 + L_4s + L_5}\,, \qquad \frac{\bar{E}_{x2}(s)}{s\Psi(s)} = \frac{s + L_2}{s^5 + L_1s^4 + L_2s^3 + L_3s^2 + L_4s + L_5}\,, \\ &\frac{\bar{E}_{x3}(s)}{s\Psi(s)} = \frac{s^2 + L_1s + L_2}{s^5 + L_1s^4 + L_2s^3 + L_3s^2 + L_4s + L_5}\,, \qquad \frac{\bar{E}_{x4}(s)}{s\Psi(s)} = \frac{s^3 + L_1s^2 + L_2s + L_3}{s^5 + L_1s^4 + L_2s^3 + L_3s^2 + L_4s + L_5}\,, \\ &\frac{\bar{E}_{x5}(s)}{s\Psi(s)} = \frac{s^4 + L_1s^3 + L_2s^2 + L_3s + L_4}{s^5 + L_1s^4 + L_2s^3 + L_3s^2 + L_4s + L_5}\,, \end{aligned} \tag{27}$$

Then, as can be seen from the expressions in Eqs. (27) and (29), for sufficiently large choices of w_0, we can force the observer state error variables to reach values that are sufficiently close to zero. Such particular characteristic, becomes more clear when taking a closed look at $E_{x4}(s)$ expression in Eq. (27):

$$\frac{\bar{E}_{x5}(s)}{s\Psi(s)} = \frac{\Psi(s) - \hat{\Psi}(s)}{s\Psi(s)} \quad \longrightarrow \quad \hat{\Psi}(s) = \frac{L_5}{s^5 + L_1s^4 + L_2s^3 + L_3s^2 + L_4s + L_5}\Psi(s)\,. \tag{28}$$

That is, the estimate $\hat{\psi}(t)$ of the generalized disturbance $\psi(t)$ can be made arbitrary precise by choosing sufficiently large values $w_0 > 0$ for the observer poles, namely:

$$\begin{aligned} &(s + w_0)^5 = s^5 + L_1s^4 + L_2s^3 + L_3s^2 + L_4s + L_5\,, \\ &L_1 = 5w_0\,,\ L_2 = 10w_0^2\,,\ L_3 = 10w_0^3\,,\ L_4 = 5w_0^4\,,\ L_5 = w_0^5\,, \end{aligned} \tag{29}$$

6.3 Closed-loop stability

Replacing the control law of Eq. (22) in Eq. (21), we have that:

$$\dddot{\bar{x}}_c + d_3\ddot{\bar{x}}_c + d_2\dot{\bar{x}}_c + d_1\bar{x}_c + d_0\bar{x}_c = d_0\bar{x}_c^* + \bar{e}_{x5} + d_3\bar{e}_{x4} + d_2\bar{e}_{x3} + d_1\bar{e}_{x2} + d_0\bar{e}_{x1}\,. \tag{30}$$

In frequency domain, we can notice that:

$$\bar{X}_c(s) = \underbrace{\frac{d_0\bar{X}_c^*(s)}{s^4 + d_3s^3 + d_2s^2 + d_1s + d_0}}_{\bar{X}_{c1}(s)} + \underbrace{\frac{d_3\bar{E}_{x4}(s) + d_2\bar{E}_{x3}(s) + d_1\bar{E}_{x2}(s) + d_0\bar{E}_{x1}(s) + \bar{E}_{x5}(s)}{s^4 + d_3s^3 + d_2s^2 + d_1s + d_0}}_{\bar{X}_{c2}(s)}\,, \tag{31}$$

in which becomes clear the term due to the set-point response $\bar{X}_{c1}(s)$ and the term due to the observer errors $\bar{X}_{c2}(s)$. For the set-point contribution, application of the *Final Value Theorem* is sufficient to reveal its steady-state response:

$$\lim_{t\to\infty}\bar{x}_{c1}(t) = \lim_{s\to 0}s\bar{X}_{c1}(s) = \lim_{s\to 0}\left(\frac{d_0\bar{x}_c^*}{s^4 + d_3s^3 + d_2s^2 + d_1s + d_0}\right) = \bar{x}_c^*\,. \tag{32}$$

For the analysis of the observer errors response $\bar{X}_{c2}(s)$, we need to use the expression in Eq. (27) in order to reach:

$$\bar{X}_{c2}(s) = \left(\frac{1}{s^4 + d_3s^3 + d_2s^2 + d_1s + d_0}\right).\left(1 - \frac{L_5}{s^5 + L_1s^4 + L_2s^3 + L_3s^2 + L_4s + L_5}\right)\Psi(s)\,. \tag{33}$$

As it is verified from Eq. (33), if $\psi(t)$ is bounded then the term $\bar{X}_{c2}(s)$ can be forced to be small enough if we choose sufficiently large values for the observer poles in Eq. (29). Thus, if the boundedness property of the function $\psi(t)$ is established then the boundedness of $\bar{x}_{c2}(t)$ and $\bar{x}_c(t)$ are guaranteed. The last conclusion will also imply the boundedness of all the closed-loop system signals.

However, before going on with the analysis, consider the definition of $\psi(t)$ in Eq. (21):

$$\psi(t) = K_s \rho_1 \dot{\alpha} + c_1 V_\alpha \,. \tag{34}$$

In a real system, the armature voltages V_α, V_β span between $\pm V_{sat}\,,\ V_{sat} > 0$. Because of this, when the motors rotate, their angular velocities $\dot{\alpha}$ and $\dot{\beta}$ will be restricted to the ranges $\pm\bar{\alpha}_{max}$ and $\pm\bar{\beta}_{max}$, respectively. That is, the limited maximum and minimum voltage levels define the highest angular velocities $\bar{\alpha}_{max}$ and $\bar{\beta}_{max}$ for both motors, in both directions of rotation. Thus, the boundedness property of function $\psi(t)$ is guaranteed and its maximum value in Eq. (34) is given by:

$$|\psi(t)| \leq \psi_{max}\,, \qquad \psi_{max} = |K_s|\rho_1 \bar{\alpha}_{max} + c_1 V_{sat}\,. \tag{35}$$

From the last expression of Eq. (35) and from Eqs. (34) and (35), it is possible to conclude that

$$\lim_{t\to\infty} \bar{x}_c(t) \approx \bar{x}_c^* \quad \longrightarrow \quad \lim_{t\to\infty} x_c(t) \approx x_c^*\,. \tag{36}$$

The boundedness property of $\psi(t)$ also implies boundeness of the observer errors $\bar{e}_{x1},\ \bar{e}_{x2},\ \bar{e}_{x3},\ \bar{e}_{x4},\ \bar{e}_{x5}$ in Eq. (27) and the estimated states $\hat{\bar{Z}}_1, \hat{\bar{Z}}_2, \hat{\bar{Z}}_3, \hat{\bar{Z}}_4, \hat{\bar{Z}}_5$ in Eq. (24), which concludes the overall analysis of the closed-loop system.

Remark 2 *Given the similarities of the dynamics of the state variables $x_c(t)$ and $y_c(t)$, in Eq. (10), the whole analysis made up to this point, regarding the system $x_c(t)$, can be reproduced to study the stability of the state variable $y_c(t)$.*

7. SMULATION RESULTS

In this section, we present and discuss the simulation results obtained with the application of the proposed method. In the following, we highlight the equations used in the simulation codes.

- Ball and plate mechanism of Eq. (3):
- The camera projection model of Eq. (4):
- The motors dynamics of Eq. (8):
- The system transformation based on Eq. (14):

$$\bar{x}_c \;=\; K_s\, x_c + V_{\alpha f}\,, \qquad \bar{y}_c \;=\; K_s\, y_c + V_{\beta f}\,. \tag{37}$$

- The filter dynamics based on Eq. (14):

$$\begin{aligned} Q_{0\alpha}(s)\ :\ \dddot{V}_{\alpha f} \;&=\; -\gamma_3 \ddot{V}_{\alpha f} - \gamma_2 \dot{V}_{\alpha f} - \gamma_1 \dot{V}_{\alpha f} - \gamma_0 V_{\alpha f} + \dot{V}_\alpha\,, \\ Q_{0\beta}(s)\ :\ \dddot{V}_{\beta f} \;&=\; -\gamma_3 \ddot{V}_{\beta f} - \gamma_2 \dot{V}_{\beta f} - \gamma_1 \dot{V}_{\beta f} - \gamma_0 V_{\beta f} + \dot{V}_\beta\,. \end{aligned} \tag{38}$$

- The control law based on Eq. (22):

$$\begin{aligned} \dot{V}_\alpha &= -\hat{\psi}_x(t) - d_3 \dddot{\hat{\bar{x}}}_c - d_2 \ddot{\hat{\bar{x}}}_c - d_1 \dot{\hat{\bar{x}}}_c - d_0 \hat{\bar{x}}_c + d_0 \bar{x}_c^*\,, \\ \dot{V}_\beta &= -\hat{\psi}_y(t) - d_3 \dddot{\hat{\bar{y}}}_c - d_2 \ddot{\hat{\bar{y}}}_c - d_1 \dot{\hat{\bar{y}}}_c - d_0 \hat{\bar{y}}_c + d_0 \bar{y}_c^*\,. \end{aligned} \tag{39}$$

- The extended observers based on Eq. (23):

$$\begin{cases} \dot{\hat{\bar{\mathbf{Z}}}}_\alpha = \mathbf{A}\hat{\bar{\mathbf{Z}}}_\alpha + \mathbf{B}\dot{V}_\alpha + \mathbf{L}e_{\bar{w}\alpha}\,, \\ \hat{\bar{w}}_\alpha = \mathbf{C}\hat{\bar{\mathbf{Z}}}_\alpha\,, \\ e_{\bar{w}\alpha} = \bar{w}_\alpha - \hat{\bar{w}}_\alpha\,, \end{cases} \qquad \begin{cases} \dot{\hat{\bar{\mathbf{Z}}}}_\beta = \mathbf{A}\hat{\bar{\mathbf{Z}}}_\beta + \mathbf{B}\dot{V}_\beta + \mathbf{L}e_{\bar{w}\beta}\,, \\ \hat{\bar{w}}_\beta = \mathbf{C}\hat{\bar{\mathbf{Z}}}_\beta\,, \\ e_{\bar{w}\beta} = \bar{w}_\beta - \hat{\bar{w}}_\beta\,. \end{cases} \tag{40}$$

The simulation was coded using MatLab/Simulink^{TM} during a time range of $12.5\ s$. The parameters used in the code were: (Ball) $m = 0.008\ Kg$, $g = 9.81\ m/s^2$, $r = 0.02\ m$, $I_b = 1.76e-5\ Kgm^2$, (camera) $f = 0.006\ m$, $\lambda = 100$, $z_0 = 1\ m$, (motors) $K_m = \bar{K}_m = 35.28$, $\sigma_1 = -\sigma_2 = -290.78$, $\rho_1 = \rho_2 = 1420.5$, (observers) $w_0 = 200$, (filters) $a = 10$, (controller) $d_0 = 625$, $d_1 = 500$, $d_2 = 150$, $d_3 = 20$. The set-points chosen for the system were the four corners of a rectangle defined in the image space which corresponds to the following cartesian space positions $[m]$: $(1)(-0.05, 0.02)$, $(2)(0.05, 0.02)$, $(3)(-0.05, -0.02)$, $(4)(0.05, -0.02)$ and $(5)(-0.05, 0.02)$. The simulation results are presented in the graphics of Figs. 4 and 5.

In Fig. 4, we noticed that the plant output converges to the four set-points as predicted by the theoretical analysis. The observer errors tend to zero very fast which enabled the control law to completly reject the *generalized disturbance term* $\psi(t)$. As can be seen in Fig. 5, saturations on motors input voltages are viewed initially due to the large error signals at the beginning, i. e. at $t = 0$. Despite such saturations, stability and convergence properties of the overall closed-loop system were verified.

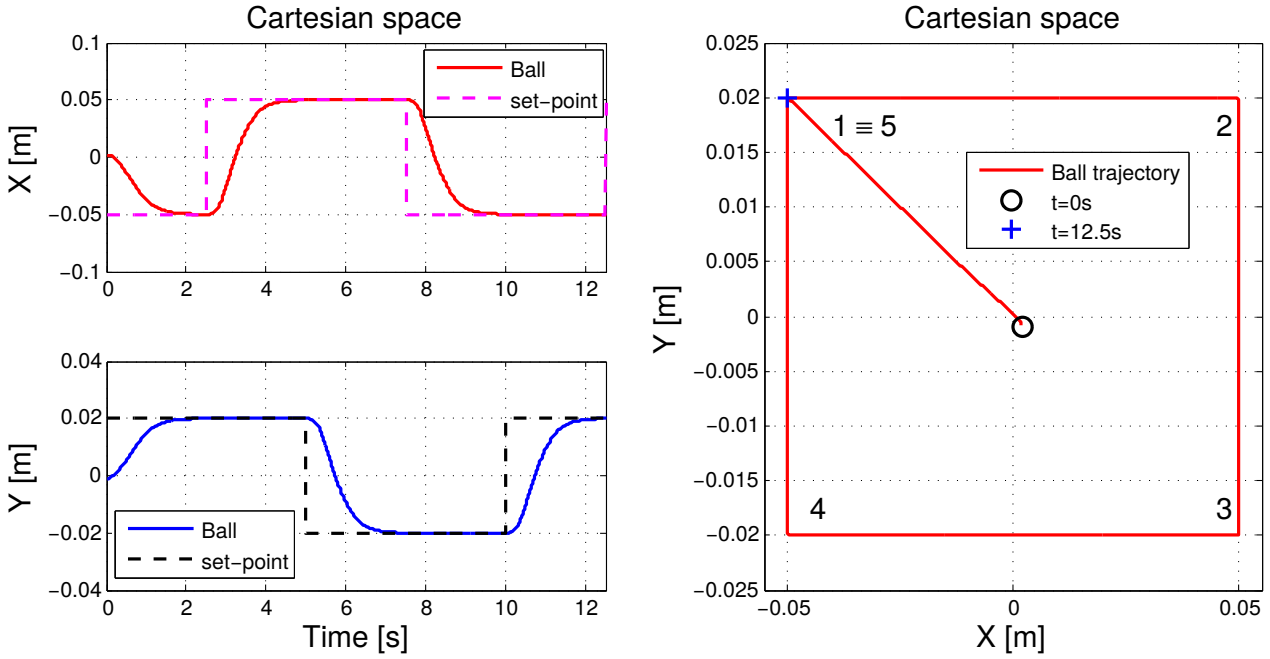

Figure 4: Simulation Results. Ball coordinates and trajectory both in cartesian space.

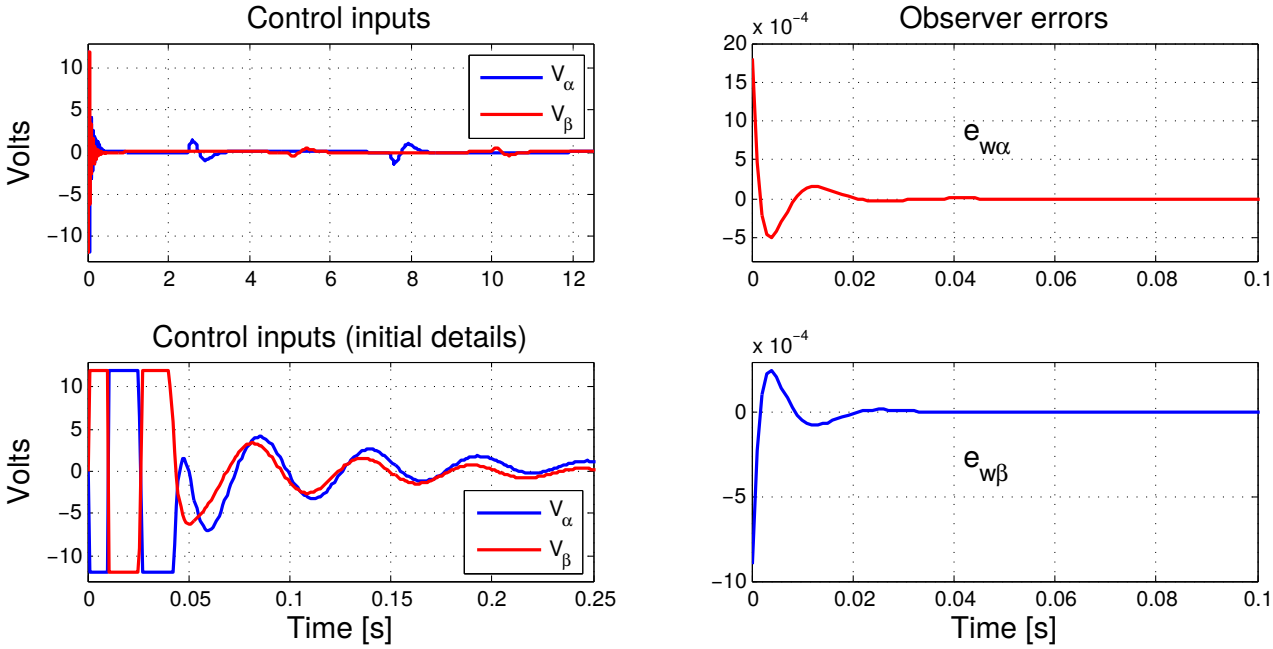

Figure 5: Simulation Results. Control signals and observer errors.

8. CONCLUSION

This work proposed a mathematical solution for the position control of a Ball and Plate mechanism with uncertain parameters, based on visual servoing and the Active Rejection Control methods. The idea of the work was to develop an extension of the ADRC controller which accounts for the uncertainty in the control gain of the plant. To solve the problem of set-point regulation of the ball, a modification in the original ADRC control scheme was proposed that consisted in the introduction of a compensator in parallel with the plant. An interesting feature of the developed strategy was the relaxation of the requirement of exact knowledge of the value of the original control gain of the plant. In this work, such requirement was reduced to the one of knowing its sign. The main contributions of the present work are (i) the exact knowledgement of system parameters, i. e., camera intrinsic parameters and motor's electromechanical constants are not required; (ii) the control synthesis is simplified due to the use of a reduced set of design constants; (iii) complexity is reduced due to the use of linear structures both on the observers and on the control laws. The stability and convergence properties of the closed loop system were proved by the theoretical demonstrations and the application of the method in a numerical simulation.

9. ACKNOWLEDGEMENTS

The authors would like to thanks the regional research agency FAPERJ (E-26/200.820/2017) and the brazilian national research agencies CNPq and CAPES for the partial financial support of the present work.

10. REFERENCES

Cheng, C.C. and Tsai, C.H., 2016. "Visual servo control for balancing a ball-plate system". *International Journal of Mechanical Engineering and Robotics Research*, Vol. 5, No. 1, p. 28.

Dorf, R.C., 2008. "Robert h". *Bishop Modern control systems Prentice Hall*.

Fan, X., Zhang, N. and Teng, S., 2004. "Trajectory planning and tracking of ball and plate system using hierarchical fuzzy control scheme". *Fuzzy Sets and Systems*, Vol. 144, No. 2, pp. 297–312.

Galvan-Colmenares, S., Moreno-Armendáriz, M.A., Rubio, J.d.J., Ortíz-Rodriguez, F., Yu, W. and Aguilar-Ibáñez, C.F., 2014. "Dual pd control regulation with nonlinear compensation for a ball and plate system". *Mathematical Problems in Engineering*, Vol. 2014.

Gao, Z., Huang, Y. and Han, J., 2001. "An alternative paradigm for control system design". In *Proceedings of the 40th IEEE Conference on Decision and Control*. IEEE, Vol. 5, pp. 4578–4585.

Han, J., 1998. "Auto-disturbance rejection control and its applications". *Control and Decision*, Vol. 13, No. 1, pp. 19–23.

Han, J., 2009. "From pid to active disturbance rejection control". *IEEE transactions on Industrial Electronics*, Vol. 56, No. 3, pp. 900–906.

Haralick, R. and Shapiro, L.G., 1993. "Computer and robot vision ii".

Kumar, P., Behera, A.K. and Bandyopadhyay, B., 2017. "Robust finite-time tracking of stewart platform: A super-twisting like observer-based forward kinematics solution". *IEEE Transactions on Industrial Electronics*, Vol. 64, No. 5, pp. 3776–3785.

Lee, K.K., Batz, G. and Wollherr, D., 2008. "Basketball robot: Ball-on-plate with pure haptic information". In *Robotics and Automation, 2008. ICRA 2008. IEEE International Conference on*. IEEE, pp. 2410–2415.

Liao, B., Lou, Y. and Li, Z., 2013. "Kinematics and optimal design of a novel 3-dof parallel manipulator for pick-and-place applications". *International Journal of Mechatronics and Automation*, Vol. 3, No. 3, pp. 181–190.

Liu, Y. and Yu, H., 2012. "Fuzzy control of an underactuated pendulum-driven cart system". *International Journal of Advanced Mechatronic Systems*, Vol. 4, No. 5-6, pp. 260–268.

Madoński, R. and Herman, P., 2011. "An experimental verification of adrc robustness on a cross-coupled aerodynamical system". In *EEE International Symposium on Industrial Electronics (ISIE)*. IEEE, pp. 859–863.

Mauro, S., Gastaldi, L., Pastorelli, S. and Sorli, M., 2016. "Dynamic flight simulation with a 3 dof parallel platform". *International Journal of Applied Engineering Research*, Vol. 11, No. 18, pp. 9436–9442.

Park, J.H. and Lee, Y.J., 2003. "Robust visual servoing for motion control of the ball on a plate". *Mechatronics*, Vol. 13, No. 7, pp. 723–738.

Rubio, J.d.J., Meléndez, F. and Figueroa, M., 2014. "An observer with controller to detect and reject disturbances". *International Journal of Control*, Vol. 87, No. 3, pp. 524–536.

Wu, J., Chen, X. and Wang, L., 2016. "Design and dynamics of a novel solar tracker with parallel mechanism". *IEEE/ASME Transactions on Mechatronics*, Vol. 21, No. 1, pp. 88–97.

Xia, Y., Pu, F., Li, S. and Gao, Y., 2016. "Lateral path tracking control of autonomous land vehicle based on adrc and differential flatness". *IEEE Transactions on Industrial Electronics*, Vol. 63, No. 5, pp. 3091–3099.

Xue, W., Bai, W., Yang, S., Song, K., Huang, Y. and Xie, H., 2015. "Adrc with adaptive extended state observer and its application to air-fuel ratio control in gasoline engines". *IEEE Transactions on Industrial Electronics*, Vol. 62, No. 9, pp. 5847–5857.

Yuan, D. and Zhang, Z., 2010. "Modelling and control scheme of the ball–plate trajectory-tracking pneumatic system with a touch screen and a rotary cylinder". *IET control theory & applications*, Vol. 4, No. 4, pp. 573–589.

Zhu, E., Pang, J., Sun, N., Gao, H., Sun, Q. and Chen, Z., 2014. "Airship horizontal trajectory tracking control based on active disturbance rejection control (adrc)". *Nonlinear Dynamics*, Vol. 75, No. 4, pp. 725–734.

11. RESPONSIBILITY NOTICE

The authors are the only responsible for the printed material included in this paper.